

Low-energy photon-photon collisions to two loops revisited

J. Gasser ^a, M.A. Ivanov ^b, M.E. Sainio ^c

^a*Institute for Theoretical Physics, University of Bern, Sidlerstrasse 5,
CH-3012 Bern, Switzerland*

^b*Laboratory of Theoretical Physics, Joint Institute for Nuclear Research,
141980 Dubna (Moscow region), Russia*

^c*Helsinki Institute of Physics, P.O. Box 64, 00014 University of Helsinki, Finland
and Department of Physical Sciences, University of Helsinki, Finland*

Abstract

In view of ongoing experimental activities to determine the pion polarizabilities, we have started to recalculate the available two-loop expressions in the framework of chiral perturbation theory, because they have never been checked before. We make use of the chiral Lagrangian at order p^6 now available, and of improved techniques to evaluate the two-loop diagrams. Here, we present the result for the neutral pions. The cross section for the reaction $\gamma\gamma \rightarrow \pi^0\pi^0$ agrees with the earlier calculation within a fraction of a percent. We present analytic results for the dipole and quadrupole polarizabilities, and compare the latter with a recent evaluation from data on $\gamma\gamma \rightarrow \pi^0\pi^0$.

PACS: 11.30.Rd; 12.38.Aw; 12.39.Fe; 13.60.Fz

Key words: Chiral perturbation theory; Two-loop diagrams; Pion polarizabilities; Compton-scattering

1 Introduction

We consider the process $\gamma\gamma \rightarrow \pi^0\pi^0$ in the framework of chiral perturbation theory (ChPT) [1,2]. The one-loop calculation of the scattering amplitude was performed in Refs. [3,4], and the two-loop amplitude was worked out in [5]. Because the effective Lagrangian at order p^6 was not available at that time, the ultraviolet divergences were evaluated in the $\overline{\text{MS}}$ scheme, then dropped and replaced with a corresponding polynomial in the external momenta. The three

new counterterms which enter at this order in the low-energy expansion were estimated with resonance saturation. Whereas such a procedure is legitimate from a technical point of view, it does not make use of the full information provided by chiral symmetry. The evaluation of the two-loop amplitude involving charged pions was performed later by Burgi [6].

Over the last ten years, considerable progress has been made in this field, both in theory and experiment. As for theory, the Lagrangian at order p^6 has been constructed [7,8], and its divergence structure has been determined [9]. This provides an important check on the above calculations: adding the counterterm contributions from the p^6 Lagrangian to the $\overline{\text{MS}}$ amplitude evaluated in [5] and in [6] must provide a scale independent result. Also in the theory, improved techniques to evaluate the two-loop diagrams that occur in these amplitudes have been developed [10]. The improvement arises mainly in the evaluation of diagrams with four external legs, where the techniques of Ref. [10] allow one to extract the ultraviolet divergences by use of simple recursion relations. We are now able to present the final result for the two-loop amplitudes in a rather compact form (in Refs. [5,6], the result was presented partly in numerical form only, because the algebraic expressions were too long to be published).

Concerning experiment, quadrupole polarizabilities [11] for the neutral pions have recently been determined from data on $\gamma\gamma \rightarrow \pi^0\pi^0$ [12]. Further, the charged pion polarizabilities $(\alpha - \beta)_{\pi^+}$ have been determined at the Mainz Microtron MAMI [13], with a result that is at variance with the two-loop calculation presented in [6]. Last but not least, there is an ongoing experiment by the COMPASS collaboration at CERN to measure the charged pion and kaon polarizabilities [14,15].

In view of these developments, and because the two-loop expressions for the polarizabilities had never been checked, we decided to recalculate these amplitudes, using the improved techniques of Ref. [10] to evaluate the integrals, and invoking the chiral Lagrangian at order p^6 [8,9]. As the calculation in the case of neutral pions involves considerably less diagrams, and because the Fortran code for these amplitudes is still available to us for checks, we have decided to start the program with a re-evaluation of these amplitudes. This is the main purpose of the present work. The evaluation of the corresponding expressions for the charged pions and for the kaons is underway and will be presented elsewhere [16].

The article is organized as follows. Section 2 contains the necessary kinematics of the process $\gamma\gamma \rightarrow \pi^0\pi^0$. To make the article self contained, we summarize in Section 3 the necessary ingredients from the effective Lagrangian framework. In Section 4, we display the Feynman diagrams and discuss their evaluation. Section 5 contains a concise representation of the two Lorentz invariant amplitudes that describe the scattering matrix element. In Section 6, we compare

the present work with the previous calculation [5], while Section 7 contains explicit expressions for the dipole and quadrupole polarizabilities valid at next-to-next-to-leading order in the chiral expansion, together with a numerical analysis and a comparison with an evaluation from data on $\gamma\gamma \rightarrow \pi^0\pi^0$ [12]. The summary and an outlook are given in Section 8. Finally, several technical aspects of the calculation are relegated to the Appendices.

2 Kinematics

The matrix element for the reaction

$$\gamma(q_1) \gamma(q_2) \rightarrow \pi^0(p_1) \pi^0(p_2) \quad (2.1)$$

is given by

$$\langle \pi^0(p_1) \pi^0(p_2) \text{ out} | \gamma(q_1) \gamma(q_2) \text{ in} \rangle = i (2\pi)^4 \delta^{(4)}(P_f - P_i) T^N, \quad (2.2)$$

with

$$T^N = e^2 \epsilon_1^\mu \epsilon_2^\nu V_{\mu\nu},$$

$$V_{\mu\nu} = i \int dx e^{-i(q_1 x + q_2 y)} \langle \pi^0(p_1) \pi^0(p_2) \text{ out} | T j_\mu(x) j_\nu(y) | 0 \rangle. \quad (2.3)$$

Here j_μ is the electromagnetic current, and $\alpha = e^2/4\pi \simeq 1/137$. We consider real photons, $q_i^2 = 0$, with $\epsilon_i \cdot q_i = 0$. The decomposition of the correlator $V_{\mu\nu}$ into Lorentz invariant amplitudes reads

$$V_{\mu\nu} = A(s, t, u) T_{1\mu\nu} + B(s, t, u) T_{2\mu\nu} + C(s, t, u) T_{3\mu\nu} + D(s, t, u) T_{4\mu\nu},$$

$$T_{1\mu\nu} = \frac{1}{2} s g_{\mu\nu} - q_{1\nu} q_{2\mu},$$

$$T_{2\mu\nu} = 2 s \Delta_\mu \Delta_\nu - \nu^2 g_{\mu\nu} - 2 \nu (q_{1\nu} \Delta_\mu - q_{2\mu} \Delta_\nu),$$

$$T_{3\mu\nu} = q_{1\mu} q_{2\nu},$$

$$T_{4\mu\nu} = s (q_{1\mu} \Delta_\nu - q_{2\nu} \Delta_\mu) - \nu (q_{1\mu} q_{1\nu} + q_{2\mu} q_{2\nu}),$$

$$\Delta_\mu = (p_1 - p_2)_\mu, \quad (2.4)$$

where

$$s = (q_1 + q_2)^2, \quad t = (p_1 - q_1)^2, \quad u = (p_2 - q_1)^2, \quad \nu = t - u \quad (2.5)$$

are the standard Mandelstam variables. The tensor $V_{\mu\nu}$ satisfies the Ward identities

$$q_1^\mu V_{\mu\nu} = q_2^\nu V_{\mu\nu} = 0. \quad (2.6)$$

The amplitudes A and B are analytic functions of the variables s, t and u , symmetric under crossing $(t, u) \rightarrow (u, t)$. The amplitudes C and D do not contribute to the process considered here, because $\epsilon_i \cdot q_i = 0$.

It is useful to introduce in addition the helicity amplitudes

$$H_{++} = A + 2(4M_\pi^2 - s)B, \quad H_{+-} = \frac{8(M_\pi^4 - tu)}{s}B. \quad (2.7)$$

The helicity components H_{++} and H_{+-} correspond to photon helicity differences $\lambda = 0, 2$, respectively. With our normalization of states $\langle \mathbf{p}_1 | \mathbf{p}_2 \rangle = 2(2\pi)^3 p_1^0 \delta^{(3)}(\mathbf{p}_1 - \mathbf{p}_2)$, the differential cross section for unpolarized photons in the centre-of-mass system is

$$\frac{d\sigma^{\gamma\gamma \rightarrow \pi^0\pi^0}}{d\Omega} = \frac{\alpha^2 s}{64} \beta(s) H(s, t), \quad H(s, t) = |H_{++}|^2 + |H_{+-}|^2, \quad (2.8)$$

with $\beta(s) = \sqrt{1 - 4M_\pi^2/s}$. The relation between the helicity amplitudes $M_{+\pm}$ in Ref. [12] and the amplitudes used here is

$$M_{++}(s, t) = 2\pi\alpha H_{++}(s, t), \quad M_{+-}(s, t) = 16\pi\alpha B(s, t). \quad (2.9)$$

The physical regions for the reactions $\gamma\gamma \rightarrow \pi^0\pi^0$ and $\gamma\pi^0 \rightarrow \gamma\pi^0$ are displayed in Fig. 1, where we also indicate with dashed lines the nearest singularities in the amplitudes A and B . These singularities are generated by two-pion intermediate states in the s, t and u channel.

3 The effective Lagrangian and its low energy constants

The effective Lagrangian consists of a string of terms. Here, we consider QCD with two flavours, in the isospin symmetry limit $m_u = m_d = \hat{m}$. At next-to-next-to-leading order (NNLO), one has

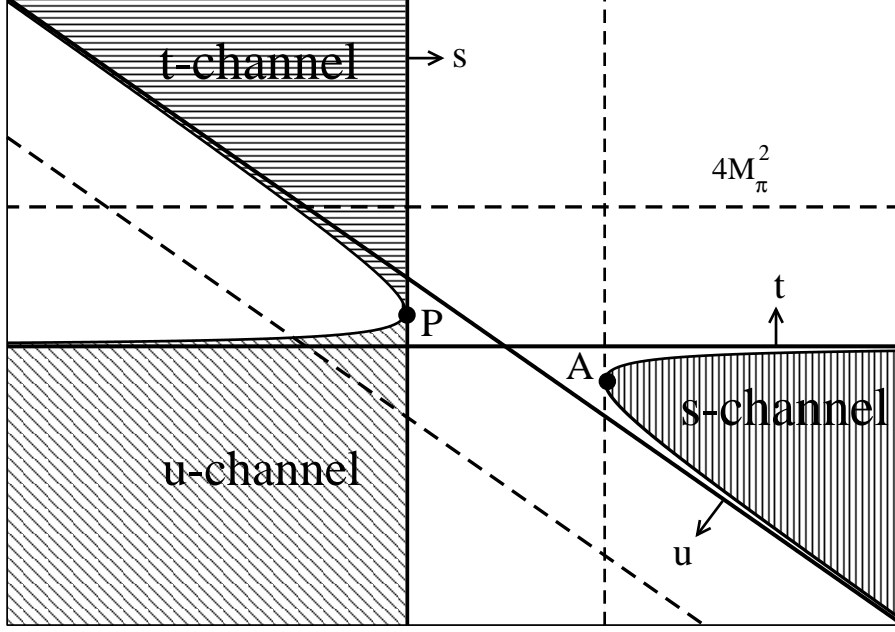


Fig. 1. Mandelstam plane with three related physical regions. s -channel: $\gamma\gamma \rightarrow \pi\pi$, t - and u -channel: $\gamma\pi \rightarrow \gamma\pi$. We denote the threshold for $\gamma\gamma \rightarrow \pi\pi$ ($\gamma\pi \rightarrow \gamma\pi$) by A (P). The dashed lines at $s, t, u = 4M_\pi^2$ indicate the presence of branch-points in the amplitude, generated by two-pion intermediate states.

$$\mathcal{L}_{\text{eff}} = \mathcal{L}_2 + \mathcal{L}_4 + \mathcal{L}_6. \quad (3.1)$$

The subscripts refer to the chiral order. The expression for \mathcal{L}_2 is

$$\mathcal{L}_2 = \frac{F^2}{4} \langle D_\mu U D^\mu U^\dagger + M^2 (U + U^\dagger) \rangle, \quad D_\mu U = \partial_\mu U - i(QU - UQ)A_\mu, \quad Q = \frac{e}{2} \text{diag}(1, -1), \quad (3.2)$$

where e is the electric charge, and A_μ denotes the electromagnetic field. The quantity F denotes the pion decay constant in the chiral limit, and M^2 is the leading term in the quark mass expansion of the pion (mass)², $M_\pi^2 = M^2(1 + O(\hat{m}))$. Further, the brackets $\langle \dots \rangle$ denote a trace in flavour space. In Eq. (3.2), we have retained only the terms relevant for the present application, i.e., we have dropped additional external fields. We choose the unitary 2×2 matrix U in the form

$$U = \sigma + i\pi/F, \quad \sigma^2 + \frac{\pi^2}{F^2} = \mathbf{1}_{2 \times 2}, \quad \pi = \begin{pmatrix} \pi^0 & \sqrt{2}\pi^+ \\ \sqrt{2}\pi^- & -\pi^0 \end{pmatrix}. \quad (3.3)$$

The Lagrangian at NLO has the structure [1]

$$\mathcal{L}_4 = \sum_{i=1}^{10} l_i K_i = \frac{l_1}{4} \langle D_\mu U D^\mu U^\dagger \rangle^2 + \dots, \quad (3.4)$$

where l_i denote low energy couplings (LECs), not fixed by chiral symmetry. At NNLO, one has [8,9]

$$\mathcal{L}_6 = \sum_{i=1}^{57} c_i P_i. \quad (3.5)$$

For the explicit expressions of the polynomials P_i , we refer the reader to Refs. [8,9]. The vertices relevant for $\gamma\gamma \rightarrow \pi^0\pi^0$ involve l_1, \dots, l_6 from \mathcal{L}_4 and c_{29}, \dots, c_{34} from \mathcal{L}_6 .

The couplings l_i and c_i absorb the divergences at order p^4 and p^6 , respectively,

$$\begin{aligned} l_i &= (\mu c)^{d-4} \{l_i^r(\mu, d) + \gamma_i \Lambda\}, \\ c_i &= \frac{(\mu c)^{2(d-4)}}{F^2} \left\{ c_i^r(\mu, d) - \gamma_i^{(2)} \Lambda^2 - (\gamma_i^{(1)} + \gamma_i^{(L)}(\mu, d)) \Lambda \right\}, \\ \Lambda &= \frac{1}{16\pi^2(d-4)}, \quad \ln c = -\frac{1}{2} \{\ln 4\pi + \Gamma'(1) + 1\}. \end{aligned} \quad (3.6)$$

The physical couplings are $l_i^r(\mu, 4)$ and $c_i^r(\mu, 4)$, denoted by l_i^r, c_i^r in the following. The coefficients γ_i are given in [1], and $\gamma_i^{(1,2,L)}$ are tabulated in [9]. In order to compare the present calculation with the result of [5], we will use the scale independent quantities \bar{l}_i introduced in [1],

$$l_i^r = \frac{\gamma_i}{32\pi^2} (\bar{l}_i + l), \quad (3.7)$$

where the *chiral logarithm* is $l = \ln(M_\pi^2/\mu^2)$. We will use [17]

$$\bar{l}_1 = -0.4 \pm 0.6, \quad \bar{l}_2 = 4.3 \pm 0.1, \quad \bar{l}_3 = 2.9 \pm 2.4, \quad \bar{l}_4 = 4.4 \pm 0.2, \quad (3.8)$$

and [18]

$$\bar{l}_\Delta \doteq \bar{l}_6 - \bar{l}_5 = 3.0 \pm 0.3. \quad (3.9)$$

The constants c_i^r occur in the combinations

$$a_1^r = 4096\pi^4 (-c_{29}^r - c_{30}^r + c_{34}^r),$$

$$\begin{aligned}
a_2^r &= 256\pi^4 (8 c_{29}^r + 8 c_{30}^r + c_{31}^r + c_{32}^r + 2 c_{33}^r) , \\
b^r &= -128\pi^4 (c_{31}^r + c_{32}^r + 2 c_{33}^r) .
\end{aligned}
\tag{3.10}$$

Their values have been estimated by resonance exchange e.g. in Ref. [5], see also [19], where c_{34}^r has been determined from a chiral sum rule. For the present application, we simply take the values obtained in [5],

$$\begin{aligned}
a_1^r(M_\rho) + 8b^r(M_\rho) &= -14 \pm 5 , \\
a_2^r(M_\rho) - 2b^r(M_\rho) &= 7 \pm 3 , \\
b^r(M_\rho) &= 3 \pm 1 ; M_\rho = 770 \text{ MeV} .
\end{aligned}
\tag{3.11}$$

In the numerical evaluations discussed later on, we use $\mu = M_\rho$. As mentioned already in Ref. [5], varying this scale between 500 MeV and 1 GeV leads to a negligible change of e.g. the cross section for the reaction $\gamma\gamma \rightarrow \pi^0\pi^0$ below 400 MeV. Finally, we will use $F_\pi = 92.4$ MeV [20] (see [21] for a recent update of this value), and $M_\pi = 135$ MeV.

4 Evaluation of the diagrams

The lowest-order contributions are the one-loop diagrams displayed in Fig. 2. They have been evaluated for the first time in Refs. [3,4], where it was noticed that the sum of these two amplitudes is ultraviolet finite, because there are no contributions from the effective Lagrangian at order p^4 at this order. The two-loop diagrams are displayed in the Figs. 3,5 and 6. The two-loop diagrams in Fig. 3 may be generated according to the scheme indicated in Fig. 4, where the shadowed blob denotes the d -dimensional elastic $\pi\pi$ -scattering amplitude at one-loop accuracy, with two pions off-shell. As is discussed in Appendix B, the one-loop integrals in the $\pi\pi$ amplitude may be represented in a dispersive manner. This allows one to reduce the two-loop integrals in Fig. 3 to the one-loop ones, where one has to perform at the end an integration over a dispersive parameter.

Two further diagrams are displayed in Fig. 5. The first one - called “acnode” in the literature - may again be evaluated by use of a dispersion relation, see Appendix B. The second one is trivial to evaluate, because it is a product of one-loop diagrams. The remaining diagrams at order p^6 are shown in Fig. 6.

The evaluation of the diagrams was done in the following manner.

- (1) We have performed the integration over the loop momenta in the d -dimensional regularization scheme, in particular using the procedure described in Ref. [10] and in Appendix B, and invoking FORM [22].

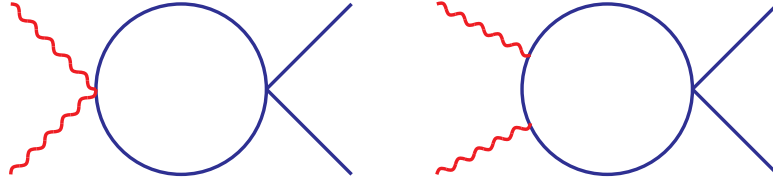


Fig. 2. The one-loop diagrams.

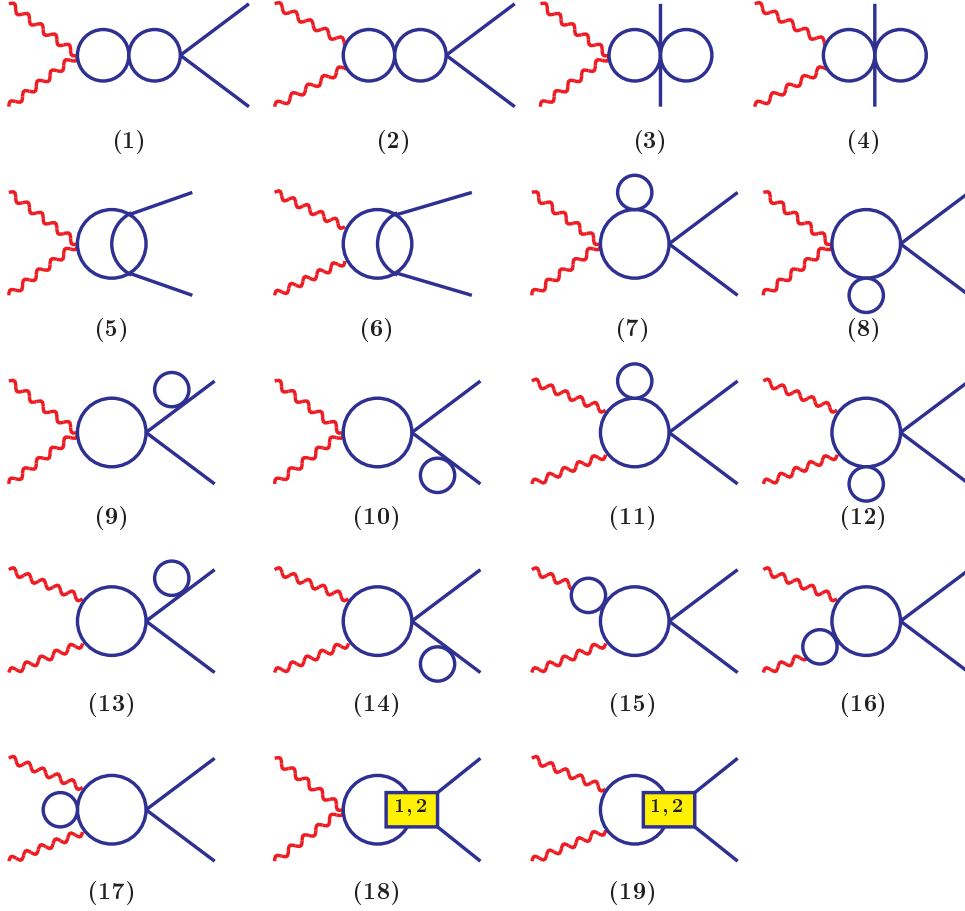


Fig. 3. A set of two-loop diagrams generated by \mathcal{L}_2 and one-loop diagrams generated by \mathcal{L}_4 .

- (2) We have then checked numerically that the amplitude satisfies the Ward identities (2.6) in d dimensions, in the unphysical region, where the amplitudes are real.
- (3) We have verified that the counterterms from the Lagrangian \mathcal{L}_6 [9] remove all ultraviolet divergences, which is a very non-trivial check on our calculation.
- (4) We have checked that the (ultra-violet finite) amplitude so obtained is scale independent.
- (5) Finally, we have numerically verified that the three lowest partial waves of

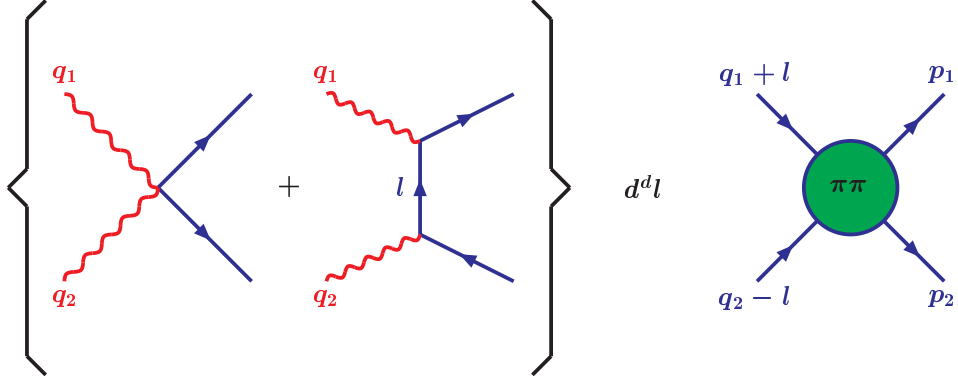


Fig. 4. Construction scheme for the diagrams in Fig. 3.

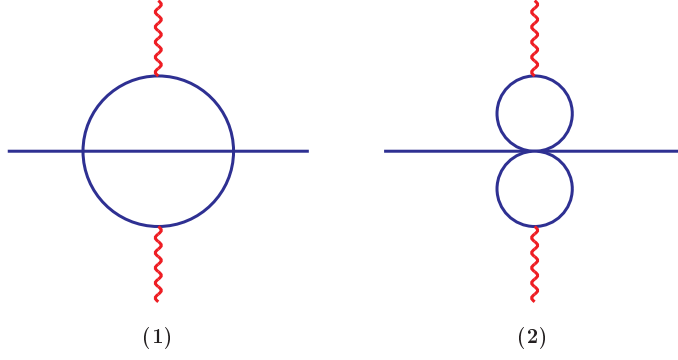


Fig. 5. Acnode and butterfly diagrams.

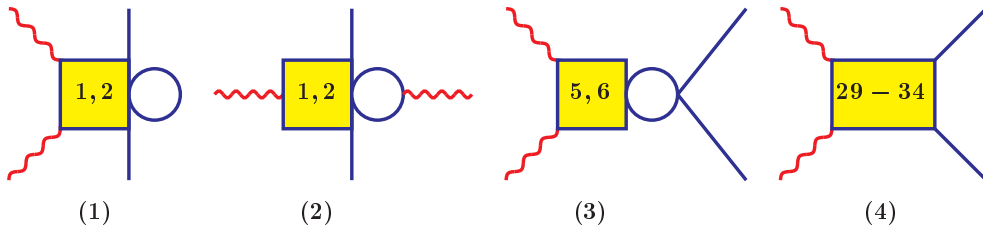


Fig. 6. The remaining diagrams at order p^6 : one-loop graphs generated by \mathcal{L}_4 , and counterterm contributions from \mathcal{L}_6 .

the helicity non-flip amplitude H_{++} carry the proper one-loop $\pi\pi$ phase, in conformity with unitarity.

We note that the steps (3) and (4) could not be performed in Refs. [5,6], because the counterterms at order p^6 were not yet available [9].

5 The two-loop amplitudes

We give the expression for the amplitudes A and B by using the same notation as in [5], and refer the reader to Appendix C of this reference for the one-loop integrals $\bar{J}(s)$, $\bar{\bar{J}}(s)$, $\bar{G}(s)$, $\bar{\bar{G}}(s)$ and $\bar{H}(s)$ that occur. We have

$$\begin{aligned} A &= \frac{4\bar{G}_\pi(s)}{sF_\pi^2}(s - M_\pi^2) + U_A + P_A + O(E^4), \\ B &= U_B + P_B + O(E^2). \end{aligned} \quad (5.1)$$

The quantity $\bar{G}_\pi(s)$ stands for $\bar{G}(s)$, evaluated with the physical pion mass. The unitary parts $U_{A(B)}$ contain s, t and u -channel cuts, and $P_{A(B)}$ are linear polynomials in s . We find

$$\begin{aligned} U_A &= \frac{2}{sF_\pi^4}\bar{G}(s) \left[(s^2 - M_\pi^4) \bar{J}(s) + C(s, \bar{l}_i) \right] + \frac{\bar{l}_\Delta}{24\pi^2 F_\pi^4} (s - M_\pi^2) \bar{J}(s) \\ &+ \frac{(\bar{l}_2 - 5/6)}{144\pi^2 s F_\pi^4} (s - 4M_\pi^2) \left\{ \bar{H}(s) + 4 \left[s \bar{G}(s) + 2M_\pi^2 (\bar{\bar{G}}(s) - 3\bar{\bar{J}}(s)) \right] d_{00}^2 \right\} \\ &+ \Delta_A(s, t, u), \\ C(s, \bar{l}_i) &= \frac{1}{48\pi^2} \left\{ 2 \left(\bar{l}_1 - \frac{4}{3} \right) (s - 2M_\pi^2)^2 + \frac{1}{3} \left(\bar{l}_2 - \frac{5}{6} \right) (4s^2 - 8sM_\pi^2 + 16M_\pi^4) \right. \\ &\left. - 3M_\pi^4 \bar{l}_3 + 12M_\pi^2 (s - M_\pi^2) \bar{l}_4 - 12sM_\pi^2 + 15M_\pi^4 \right\}, \\ d_{00}^2 &= \frac{1}{2}(3 \cos^2 \theta - 1), \end{aligned} \quad (5.2)$$

$$U_B = \frac{(\bar{l}_2 - 5/6) \bar{H}(s)}{288\pi^2 F_\pi^4 s} + \Delta_B(s, t, u). \quad (5.3)$$

The expressions for $\Delta_{A(B)}$ are displayed in the Appendices C and D.

The polynomial parts are

$$\begin{aligned} P_A &= \frac{1}{(16\pi^2 F_\pi^2)^2} \left[a_1 M_\pi^2 + a_2 s \right], \\ a_1 &= a_1^r + \frac{1}{18} \left\{ 4l^2 + l \left(8\bar{l}_2 + 12\bar{l}_\Delta - \frac{4}{3} \right) - \frac{20}{3} \bar{l}_2 + 12\bar{l}_\Delta + \frac{110}{9} \right\}, \\ a_2 &= a_2^r - \frac{1}{18} \left\{ l^2 + l \left(2\bar{l}_2 + 12\bar{l}_\Delta - \frac{4}{3} \right) - \frac{5}{3} \bar{l}_2 + 12\bar{l}_\Delta + \frac{697}{144} \right\}, \end{aligned} \quad (5.4)$$

$$\begin{aligned}
P_B &= \frac{b}{(16 \pi^2 F_\pi^2)^2}, \\
b &= b^r - \frac{1}{36} \left[l^2 + l \left(2 \bar{l}_2 + \frac{2}{3} \right) - \frac{1}{3} \bar{l}_2 + \frac{393}{144} \right], \\
l &= \log \frac{M_\pi^2}{\mu^2}.
\end{aligned} \tag{5.5}$$

The constants a_1^r, a_2^r and b^r are displayed in terms of the LECs at order p^6 in Eq. (3.10). Using the fact that the bare couplings c_i displayed in Eq. (3.6) are scale independent, one indeed finds that the above expressions for the amplitudes A, B are scale independent as well.

6 Comparison with the previous calculation

We can now compare the amplitudes A, B with the earlier calculation, presented in Section 7 of Ref. [5]. In that reference, the amplitudes were evaluated with a different techniques. Furthermore, the Lagrangian \mathcal{L}_6 was not available in those days, and an important ingredient to check the final result was, therefore, missing. We can make the following observations.

- (1) The amplitudes A and B consist of a part with explicit analytic expressions, and additional terms $\Delta_{A,B}$, that are given in the Appendices C and D of the present work in the form of integrals over Feynman parameters. These latter terms were given only in numerical form in [5].
- (2) The explicit analytic expressions agree with the previous calculation, except for the coefficient of the single logarithm in a_2 in Eq. (5.4). The factor $2/3$ in [5] is replaced by $-4/3$ here. As the present amplitude is scale independent, we conclude that it is the result Eq. (5.4) which is correct¹. This mistake does not affect the algebraic expressions for the polarizabilities discussed below, for which we fully agree with Ref. [5].
- (3) We can compare the quantities $\Delta_{A,B}$ in numerical form only. For this purpose, we have made two checks. First, we have evaluated the cross section for the reaction $\gamma\gamma \rightarrow \pi^0\pi^0$ below a centre-of-mass energy of 400 MeV, using the same values for the LECs as in [5]. It agrees with the previous one within a fraction of a percent - the difference would not be visible in Fig. 5 of Ref. [5], and we do not, therefore, reproduce that plot here. Second, we have re-evaluated the two-loop contributions to the polarizabilities presented in column 4 of Table 3 in [5]. The numbers (0.17, - 0.31) in the old calculation become (0.17, - 0.30) here.

¹ Burgi [23] provides in his thesis work the isospin $I = 0, 2$ amplitudes, and the one for the charged pions. Subtracting the latter from the former reveals that his calculation agrees with the statement just made.

- (4) To summarize, we confirm the previous result up to the coefficient in one of the chiral logarithms, and up to minute changes in the numerical values of $\Delta_{A,B}$. Numerically, the results in [5] are not affected in any significant manner by these modifications, whose effect is by far smaller than the uncertainties generated by the (not precisely known) values of the low energy constants.

7 Pion polarizabilities: dipole and quadrupole

The *dipole* and *quadrupole* polarizabilities are defined [11,12] through the expansion of the helicity amplitudes at fixed $t = M_\pi^2$,

$$\frac{\alpha}{M_\pi} H_{+\mp}(s, t = M_\pi^2) = (\alpha_1 \pm \beta_1)_{\pi^0} + \frac{s}{12} (\alpha_2 \pm \beta_2)_{\pi^0} + \mathcal{O}(s^2). \quad (7.1)$$

Because we have at our disposal the helicity amplitudes at two-loop order, we can work out the polarizabilities to the same accuracy. It turns out that all relevant integrals can be performed in closed form. We discuss the results in the remaining part of this Section.

7.1 Chiral expansion

Using the same notation as in [5], we find for the *dipole* polarizabilities

$$(\alpha_1 \pm \beta_1)_{\pi^0} = \frac{\alpha}{16 \pi^2 F_\pi^2 M_\pi} \left\{ c_{1\pm} + \frac{M_\pi^2 d_{1\pm}}{16 \pi^2 F_\pi^2} + \mathcal{O}(M_\pi^4) \right\}, \quad (7.2)$$

with

$$\begin{aligned} c_{1+} &= 0, c_{1-} = -1/3, \\ d_{1+} &= 8b^r - \frac{1}{648} (144l(l + 2\bar{l}_2) + 96l + 288\bar{l}_2 + 113 + \Delta_+), \\ d_{1-} &= a_1^r + 8b^r + \frac{1}{648} (144l(3\bar{l}_\Delta - 1) + 36(8\bar{l}_1 - 3\bar{l}_3 - 12\bar{l}_4 + 12\bar{l}_\Delta) \\ &\quad + 43 + \Delta_-), \\ \Delta_+ &= 13643 - 1395\pi^2, \Delta_- = -3559 + 351\pi^2. \end{aligned} \quad (7.3)$$

We have split off the numbers 113 and 43, respectively, to illustrate that these expressions completely agree with the ones displayed in Eq. (8.14) of Ref. [5],

Table 1

The dipole and quadrupole polarizabilities in units of 10^{-4} fm^3 and 10^{-4} fm^5 , respectively. The symbol [*] refers to the present work. The slight difference in the value of $(\alpha_1 + \beta_1)_{\pi^0}$ with the one reported in [5] is due to the updated values of \bar{l}_2 and of the pion decay constant F_π used here.

	ChPT	dispersion relations
$(\alpha_1 - \beta_1)_{\pi^0}$	-1.9 ± 0.2 [5]	-1.6 ± 2.2 [24]
$(\alpha_1 + \beta_1)_{\pi^0}$	1.1 ± 0.3 [5]	0.98 ± 0.03 [24] 1.00 ± 0.05 [25]
$(\alpha_2 - \beta_2)_{\pi^0}$	37.6 ± 3.3 [*]	39.70 ± 0.02 [12]
$(\alpha_2 + \beta_2)_{\pi^0}$	0.04 [*]	-0.181 ± 0.004 [12]

where, as already mentioned, no explicit expressions for the remainders $\Delta_{+,-}$ were worked out. For the *quadrupole* polarizabilities, we obtain

$$(\alpha_2 \pm \beta_2)_{\pi^0} = \frac{\alpha}{16 \pi^2 F_\pi^2 M_\pi^3} \left\{ c_{2\pm} + \frac{M_\pi^2 d_{2\pm}}{16 \pi^2 F_\pi^2} + O(M_\pi^4) \right\}, \quad (7.4)$$

with

$$c_{2+} = 0, \quad c_{2-} = 156/45, \\ d_{2+} = -\frac{5009}{27} + \frac{13453 \pi^2}{720} + \frac{16 \bar{l}_2}{45}, \quad (7.5)$$

$$d_{2-} = 12 a_2^r - 24 b^r + \frac{1}{960} \left(1280 l (1 - 6 \bar{l}_\Delta) + 19216 - 1811 \pi^2 \right) \\ - \frac{4 (52 \bar{l}_1 + 5 \bar{l}_2 + 3 \bar{l}_3 - 78 \bar{l}_4 + 105 \bar{l}_\Delta)}{45}. \quad (7.6)$$

7.2 Numerical results

For numerical evaluations of the polarizabilities we use the values of the LECs given in Section 3. The results are displayed in Table 1, where we also quote the results from dispersive calculations. The following comments are in order.

- (1) The slight difference in the value of $(\alpha_1 + \beta_1)_{\pi^0}$ with the one reported in [5] is due to the updated values of \bar{l}_2 and of the pion decay constant F_π used here.

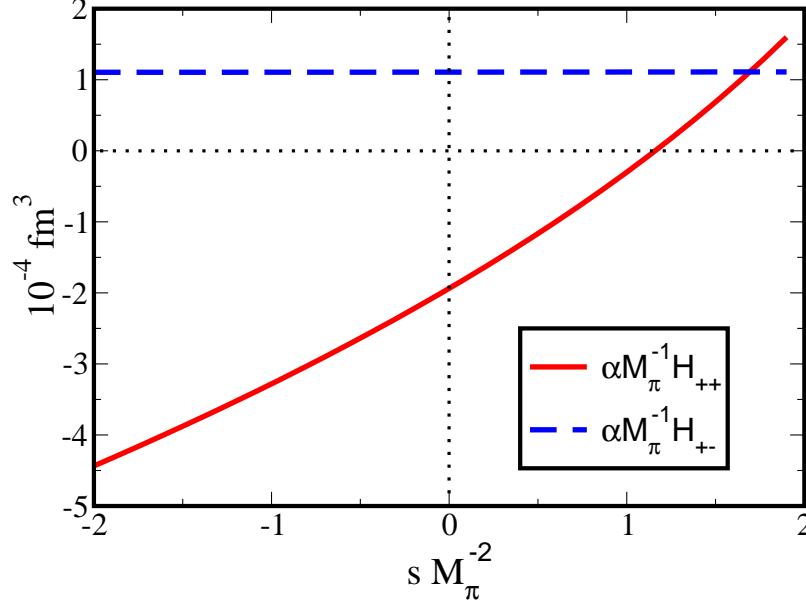


Fig. 7. The helicity amplitudes $\frac{\alpha}{M_\pi} H_{++}(s, t = M_\pi^2)$ (solid line), $\frac{\alpha}{M_\pi} H_{+-}(s, t = M_\pi^2)$ (dashed line), plotted as a function of s , at $t = M_\pi^2$. Compare with the definition of the polarizabilities in Eq. (7.1) The dotted lines are displayed to guide the eye.

- (2) Our results for the dipole polarizabilities as well as for the quadrupole polarizabilities $(\alpha_2 - \beta_2)_{\pi^0}$ agree with the results of the recent investigations performed in [25,24] and [12] within the uncertainties quoted.
- (3) The prediction for the quadrupole polarizability $(\alpha_2 + \beta_2)_{\pi^0}$ is positive, in contrast to the result reported in Ref. [12]. The ChPT expression contains as the only LEC \bar{l}_2 , known rather accurately from $\pi\pi$ scattering [17]. We come back to this point in the following subsection, where we also discuss the uncertainties quoted in the Table for the ChPT calculation.
- (4) We plot the helicity amplitudes in Fig. 7. It illustrates the fact that the helicity flip amplitude H_{+-} is quite flat at this order, in contrast to the non-flip amplitude H_{++} , see the values of the quadrupole polarizabilities in Table 1.
- (5) For a comparison of the ChPT - predictions of the dipole polarizabilities with calculations performed before 1994, and for additional information on these quantities, we refer the interested reader to Refs. [5] and [26].

7.3 Estimating the uncertainties

To estimate the uncertainties in the prediction of the polarizabilities, we first note that the helicity non-flip amplitude H_{++} starts out at order p^4 . We have therefore, for this quantity, a leading and next-to-leading order calculation at our disposal. For the corresponding polarizabilities $(\alpha_1 - \beta_1)_{\pi^0}$ and $(\alpha_2 - \beta_2)_{\pi^0}$, we thus simply add in quadrature the uncertainties generated by the order p^4

and p^6 LECs (see Section 3). The resulting numbers are given in column 2 of Table 1. They do not incorporate an estimate of the higher order contributions.

On the other hand, the helicity flip amplitude H_{+-} starts out at order p^6 , and we have determined here only its leading order term. According to Eq. (2.7), this amplitude is proportional to $B(s, t, u)$, which is an analytic function of the variables s, ν at the Compton threshold and can be, therefore, expanded in a Taylor series,

$$B(s, t, u) = U + Vs + W\nu^2 + \mathcal{O}(s^2, \nu^4, s\nu^2). \quad (7.7)$$

The relation to the polarizabilities is

$$(\alpha_1 + \beta_1)_{\pi^0} = 8\alpha M_\pi U, \quad (\alpha_2 + \beta_2)_{\pi^0} = 96\alpha M_\pi V. \quad (7.8)$$

The Taylor coefficients themselves have a chiral expansion of the form

$$\begin{aligned} U &= \frac{1}{(16\pi^2 F_\pi^2)^2} \left[U_0 + \frac{M_\pi^2 U_1}{16\pi^2 F_\pi^2} + \mathcal{O}(M_\pi^4) \right], \\ V &= \frac{1}{(16\pi^2 F_\pi^2)^2 M_\pi^2} \left[V_0 + \frac{M_\pi^2 V_1}{16\pi^2 F_\pi^2} + \mathcal{O}(M_\pi^4) \right]. \end{aligned} \quad (7.9)$$

Whereas LECs from order p^6 do contribute to U_0 , the leading term V_0 is a pure loop effect, because V_0/M_π^2 is not analytic in the pion mass and thus cannot receive contributions from polynomial counterterms. To illustrate this point, and to estimate the size of V_1 , we consider the vector meson exchange amplitudes worked out in [5]. The contribution from ω exchange is dominant and given by

$$B_\omega(s, t, u) = \frac{C_\omega}{2} \left[\frac{1}{M_\omega^2 - t} + \frac{1}{M_\omega^2 - u} \right]; \quad C_\omega = 0.67 \text{ GeV}^{-2}. \quad (7.10)$$

In the language of ChPT, this amplitude starts out at order p^6 . It does contribute to U_0 - this term is included in the resonance exchange estimates for the $\mathcal{O}(p^6)$ LECs in (3.11). For this reason, we calculate the uncertainties in $(\alpha_1 + \beta_1)_{\pi^0}$ as before, with a result that is given in the second row of Table 1. Again, it does not incorporate an estimate of higher order contributions.

Finally, we come to the estimate of the uncertainty in $(\alpha_2 + \beta_2)_{\pi^0}$. In agreement with what is said above, resonance exchange does not contribute to V_0 . On the other hand, there is no reason why this term should dominate the contribution from V_1 . Indeed, if we use (7.10) to also estimate effects from order p^8 , we find with $M_\omega = 782 \text{ MeV}$ the value $V_1 = -2.2$. The corresponding contribution

to the quadrupole polarizability $(\alpha_2 + \beta_2)_{\pi^0}$ is $-0.25 \cdot 10^{-4} \text{ fm}^5$ - of the order needed to bring the ChPT calculation into agreement with the analysis of Ref. [12].

This result illustrates that the discrepancy between the chiral prediction for the quadrupole polarizability $(\alpha_2 + \beta_2)_{\pi^0}$ at order p^6 and the dispersion analysis in Ref. [12] is of no significance, because the terms neglected may well be much larger than the leading order term, which would only dominate for very small values of the pion mass. On the other hand, to obtain a reliable estimate of $(\alpha_2 + \beta_2)_{\pi^0}$ in the framework of ChPT, one needs to perform a reliable calculation of the relevant couplings at order p^8 . This is outside the scope of the present work. For this reason, we do not quote an uncertainty for $(\alpha_2 + \beta_2)_{\pi^0}$ in Table 1.

8 Summary and outlook

- (1) We have recalculated the two-loop expression for the amplitude $\gamma\gamma \rightarrow \pi^0\pi^0$ in the framework of chiral perturbation theory. We have made use of the techniques developed in Ref. [10], and of the effective Lagrangian \mathcal{L}_6 available now [8,9].
- (2) The method has allowed us to evaluate the dipole and quadrupole polarizabilities in closed form. [As far as we are aware, the quadrupole polarizabilities have never been calculated in ChPT before.] The two Lorentz invariant amplitudes A and B are presented as a sum over multiple integrals over Feynman parameters whose numerical evaluation poses no difficulty. This is in contrast to Ref. [5], where part of the amplitudes, denoted by $\Delta_{A,B}$, were published in numerical form only.
- (3) Our result agrees with the earlier calculation [5] up to the coefficient in one of the chiral logarithms in the amplitude A , and up to minute differences in the numerical values of the remainder $\Delta_{A,B}$. The induced changes in the numerics of the cross section and of the dipole polarizabilities are far below the uncertainties generated by the (not precisely known) values of the low energy constants.
- (4) The values for the dipole and quadrupole polarizabilities are presented in Table 1 and confronted with recent evaluations from data on $\gamma\gamma \rightarrow \pi^0\pi^0$. There is reasonable agreement for the dipole polarizabilities. As for the quadrupole ones, the combination $(\alpha_2 - \beta_2)_{\pi^0}$ related to the helicity non-flip amplitude agrees with [12] within the uncertainties quoted. On the other hand, the sum $(\alpha_2 + \beta_2)_{\pi^0}$ - related to the helicity flip amplitude - differs in sign from the one in Ref. [12]. We have shown why this does not contradict the predictions of ChPT : this quantity is a two-loop effect, and one expects from order p^8 (three loops) substantial corrections to the leading order result. We have indeed identified ω -exchange as an

important contribution at this order.

- (5) It would be instructive to improve the estimates for the LECs c_{29}, \dots, c_{34} in the sense that in these estimates, the constraints from the asymptotics of QCD [27,19] should be respected.

The corresponding calculation of the charged pion polarizabilities is in progress [16].

Acknowledgements

This work was completed while M.A.I. visited the University of Bern. It is a pleasure to thank G. Colangelo, J. Bijnens and B. Moussallam for useful discussions, and S. Bellucci for useful remarks concerning the manuscript. This work was supported by the Swiss National Science Foundation, by RTN, BBW-Contract No. 01.0357, and EC-Contract HPRN-CT2002-00311 (EURIDICE). M.A.I. also appreciates the partial support by the Russian Fund of Basic Research under Grant No. 04-02-17370. Also, partial support by the Academy of Finland, grant 54038, is acknowledged.

A Notation

In order to simplify the expressions, we set the pion mass equal to one in all Appendices,

$$M_\pi = 1. \quad (\text{A.1})$$

We use the following notation for d -dimensional one-loop and two-loop integrals,

$$\langle \dots \rangle = \int \frac{d^d l}{(2\pi)^d i} (\dots), \quad \langle \langle \dots \rangle \rangle = \int \frac{d^d l_1}{(2\pi)^d i} \int \frac{d^d l_2}{(2\pi)^d i} (\dots). \quad (\text{A.2})$$

In particular,

$$\left\langle \frac{1}{[z - l^2]^n} \right\rangle = F_n[z], \quad n \geq 1, \\ F_n[z] = z^{w+2-n} C(w) \frac{\Gamma(n-2-w)}{\Gamma(n)}, \quad w = \frac{d}{2} - 2. \quad (\text{A.3})$$

The measures in the integration over Feynman parameters are defined by

$$d^2x = dx_2 dx_3, \quad d^3x = dx_1 dx_2 dx_3. \quad (\text{A.4})$$

In dispersion relations, we use the d -dimensional measure

$$\begin{aligned} [d\sigma] &= \frac{C(w) \Gamma(3/2)}{\Gamma(3/2 + w)} \left(\frac{\sigma}{4} - 1 \right)^w \beta d\sigma, \\ C(w) &= \frac{1}{(4\pi)^{2+w}}, \quad \beta = \sqrt{1 - 4/\sigma}. \end{aligned} \quad (\text{A.5})$$

B The acnode

The evaluation of the two-loop vertex and box diagrams (5) and (6) in Fig. 3 is described in Ref. [10]. It is based on a d -dimensional dispersive representation of the fish-type diagram,

$$\begin{aligned} J(p^2) &= \left\langle \frac{1}{[1 - l^2][1 - (l + p)^2]} \right\rangle = C(w) \Gamma(-w) \int_0^1 dx [1 - p^2 x(1 - x)]^w \\ &= \int_4^\infty \frac{[d\sigma]}{\sigma - p^2}; \quad -1.5 < \omega < 0, \end{aligned} \quad (\text{B.1})$$

where the measure $[d\sigma]$ is given in Appendix A. This representation allows one to reduce the two-loop vertex and box integrals to the one-loop case, with a final integration over the dispersion parameter σ . The ultraviolet divergences can be extracted by invoking recursion relations [10]. While the acnode was treated in a different manner in [10], we evaluate it here analogously to the vertex and box diagrams just mentioned. This results in considerable simplifications in the numerical programs. For this purpose, we invoke a dispersion relation for the function $I(m, n; s)$ defined by

$$I(m, n; s) = \int_0^1 dx [1 - s x(1 - x)]^m [x(1 - x)]^n, \quad -1 < m < 0. \quad (\text{B.2})$$

$I(m, n; s)$ is analytic in the complex s -plane, cut along the real axis for $\text{Re } s \geq 4$. To evaluate its absorptive part, we observe that the imaginary part of

the first factor of the integrand in Eq. (B.2), evaluated at the upper rim of the cut, is

$$\begin{aligned} \text{Im} [1 - s x (1 - x)]^m &= -\sin(\pi m) [s x (1 - x) - 1]^m, \\ s > 4 \quad x_- < x < x_+, \quad x_{\pm} &= (1/2) \left(1 \pm \sqrt{1 - 4/s} \right). \end{aligned} \quad (\text{B.3})$$

The integrand is symmetric around $x = 1/2$, so we may restrict the integration from x_- to $1/2$ in the evaluation of the absorptive part of $I(m, n; s)$. The substitution $x = (1/2) \left(1 - \sqrt{(1 - 4/s)(1 - u)} \right)$ generates a hypergeometric function, and we arrive at the dispersion relation

$$\begin{aligned} I(m, n; s) &= \int_4^{\infty} \frac{d\sigma \rho(m, n; \sigma)}{\sigma - s}, \\ \rho(m, n; \sigma) &= \frac{\Gamma(3/2) \delta^{1/2+m}}{4^n \Gamma(3/2 + m) \Gamma(-m)} {}_2F_1 \left(\frac{1}{2}, \frac{3}{2} + m + n; \frac{3}{2} + m; -\delta \right), \\ \delta &= \frac{\sigma}{4} - 1. \end{aligned} \quad (\text{B.4})$$

In particular, we find

$$\begin{aligned} \rho(m, 0; \sigma) &= \frac{\Gamma(3/2) \beta \delta^m}{\Gamma(3/2 + m) \Gamma(-m)}, \\ \rho(m, 1; \sigma) &= \frac{\Gamma(3/2) \beta \delta^m}{4 \Gamma(5/2 + m) \Gamma(-m)} \left(1 + m + \frac{2}{\sigma} \right), \\ \rho(m, 2; \sigma) &= \frac{\Gamma(3/2) \beta \delta^m}{16 \Gamma(7/2 + m) \Gamma(-m)} \left(2 + 3m + m^2 + \frac{4(1+m)}{\sigma} + \frac{12}{\sigma^2} \right), \end{aligned} \quad (\text{B.5})$$

with β given by Eq. (A.5).

The dispersion relation (B.4) allows us to evaluate the integral that occurs in the evaluation of the acnode diagram (1) in Fig. 5,

$$A_N^{\mu\nu} = \left\langle \left\langle \frac{4 l_1^\mu l_2^\nu V_L V_R}{D_1 D_2 D_3 D_4 D_5} \right\rangle \right\rangle,$$

$$\begin{aligned} V_L &= (l_2 + q_2 - l_1)^2 - 1, \\ V_R &= (l_1 + q_1 - l_2)^2 - 1, \\ D_1 &= 1 - l_1^2, \quad D_2 = 1 - (l_1 + q_1)^2, \end{aligned}$$

$$\begin{aligned}
D_3 &= 1 - l_2^2, & D_4 &= 1 - (l_2 + q_2)^2, \\
D_5 &= 1 - (l_1 - l_2 - p_1 + q_1)^2.
\end{aligned} \tag{B.6}$$

We combine $1/(D_1 D_2)$ and $1/(D_3 D_4)$ by using x_1 and x_2 as Feynman parameters, respectively. By shifting l_1 and l_2 and again dropping terms that vanish upon contraction with the polarization vectors, one obtains

$$\begin{aligned}
A_N^{\mu\nu} &= \int_0^1 d^2x \left\langle \left\langle \frac{l_2^\nu}{[1 - l_2^2]^2} \cdot \frac{l_1^\mu P_N(l_i, p_i, q_i)}{[1 - l_1^2]^2 [1 - (l_1 - r)^2]} \right\rangle \right\rangle, \\
r &= l_2 - q, & q &= x_1 q_1 + x_2 q_2 - p_1.
\end{aligned} \tag{B.7}$$

Here, $P_N(l_i, p_i, q_i)$ is a polynomial in the momenta indicated. The integration over l_1 is performed by using the dispersion relation (B.4) with $s = r^2$. Then we proceed in a manner which is similar to the case of the box diagram described in Ref. [10]. The final expression can be written as a combination of the integrals

$$\begin{aligned}
A(i, k, m, n) &= \int_4^\infty [d\sigma] \int_0^1 d^3x \left(\frac{\sigma}{4} - 1 \right)^{1-i} \sigma^{-k} (1 - x_3)^m F_n[z_{\text{acn}}], \\
z_{\text{acn}} &= x_3^2 + (1 - x_3) \sigma - x_3 (1 - x_3) a, \\
a &= x_1 x_2 s + x_1 (t - 1) + x_2 (u - 1),
\end{aligned} \tag{B.8}$$

where $F_n[z]$ is defined in (A.3). The integrals $A(i, k, m, n)$ are convergent at $w = 0$ in the case

$$\begin{aligned}
i &= 1, & k &= 0, & m &\geq 1, & n &\geq 4, \\
i &= 1, & k &\geq 1, & m &\geq 1, & n &\geq 3, \\
i &= 2, & k &\geq 0, & m &\geq 0, & n &\geq 3.
\end{aligned}$$

To single out the divergent part in the remaining integrals, we invoke recursion relations in the following manner. We perform a partial integration in x_3 , and use

$$\int dx_3 (1 - x_3)^m = -\frac{(1 - x_3)^{m+1}}{m+1}.$$

Then we express $(1 - x_3) \sigma$ through z_{acn} and obtain

$$\begin{aligned}
(m + 3 - n + \omega) A(i, k, m, n) &= \\
\text{Div}(i, k, n) - n [A(i, k, m, n + 1) - (1 + a) A(i, k, m + 2, n + 1)] &, \tag{B.9}
\end{aligned}$$

where

$$\begin{aligned}
\text{Div}(i, k, n) &= 4^{3-n-k+\omega} \frac{C^2(w) \Gamma(3/2)}{\Gamma(3/2 + \omega)} \frac{\Gamma(n-2-\omega)}{\Gamma(n)} \times \\
&\quad B(5/2 - i + \omega, n + k - 4 + i - 2\omega), \\
B(x, y) &= \frac{\Gamma(x)\Gamma(y)}{\Gamma(x+y)}.
\end{aligned} \tag{B.10}$$

The divergences in $\text{Div}(i, k, n)$ can be worked out straightforwardly.

The integral $A(1, 0, 0, 3)$ must be considered separately. We write

$$\begin{aligned}
A(1, 0, 0, 3) &= D(0, 3) + \int_4^\infty [d\sigma] \int_0^1 d^3x \{F_3[z_{\text{acn}}] - F_3[y]\}, \\
y &= x_3^2 + (1 - x_3) \sigma.
\end{aligned} \tag{B.11}$$

The divergent quantity $D(0, 3)$ is worked out in Appendix C.1 of Ref. [10], whereas the integral on the right-hand side is convergent at $d = 4$.

This concludes our discussion of the acnode integral (B.7).

C The quantities Δ_A and Δ_B

Here we display the expressions for the quantities $\Delta_{A(B)}$ in Eqs. (5.2) and (5.3).

$$\begin{aligned}
\Delta_A(s, t, u) &= \frac{1}{(4\pi F_\pi)^4} \left\{ \left(\frac{689}{162} - \frac{4\pi^2}{9} \right) + \frac{15043}{64800} s \right\} \\
&+ \frac{1}{(4\pi F_\pi)^4} \frac{1}{288} \left\{ F_A^{\text{acn}}(s, t, u) + F_A^{\text{ver}}(s) + F_A^{\text{box}}(s, t, u) \right\},
\end{aligned} \tag{C.1}$$

$$\begin{aligned}
\Delta_B(s, t, u) &= \frac{1}{(4\pi F_\pi)^4} \left\{ \frac{8329}{43200} + \left(\frac{2987}{1350} - \frac{2\pi^2}{9} \right) \frac{1}{s} \right\} \\
&+ \frac{1}{(4\pi F_\pi)^4} \frac{1}{288} \left\{ F_B^{\text{acn}}(s, t, u) + F_B^{\text{ver}}(s) + F_B^{\text{box}}(s, t, u) \right\},
\end{aligned} \tag{C.2}$$

where

$$F_I^{\text{acn}} = \int_4^\infty d\sigma \beta \int_0^1 d^3x \left\{ \left[\frac{P_{I;\text{acn}}^{(0)}}{y} + \frac{P_{I;\text{acn}}^{(1)}}{\sigma} \right] \frac{1}{z_{\text{acn}}} + \frac{P_{I;\text{acn}}^{(2)}}{z_{\text{acn}}^2} \right\},$$

$$\begin{aligned}
F_I^{\text{ver}} &= \int_4^\infty \frac{d\sigma}{\sigma} \beta \int_0^1 d^2x \cdot \frac{P_{I;\text{ver}}}{z_{\text{ver}}} , \\
F_I^{\text{box}} &= \int_4^\infty \frac{d\sigma}{\sigma} \beta \int_0^1 d^3x \sum_{n=1}^2 \left\{ P_{I;\text{box}+}^{(n)} D_{\text{box}+}^{(n)} + P_{I;\text{box}-}^{(n)} D_{\text{box}-}^{(n)} \right\} ; \ I = A, B ,
\end{aligned} \tag{C.3}$$

and

$$D_{\text{box}\pm}^{(n)} = \frac{1}{zn_{\text{box};\text{t}}} \pm \frac{1}{z_{\text{box};\text{u}}^n} .$$

Here P_I are polynomials in $s, \nu = t - u$ and in x_i . Their explicit expressions are given in Appendix D. The quantity z_{acn} is displayed in Eq. (B.8), y is given in (B.11), and

$$\begin{aligned}
z_{\text{ver}} &= \sigma (1 - x_3) + x_3^2 y_2, & y_2 &= 1 - s x_2 (1 - x_2), \\
z_{\text{box};\text{t}} &= B_{\text{t}} - A_{\text{t}} x_1, \\
A_{\text{t}} &= x_2 x_3 [s (1 - x_2) x_3 + (1 - t) (1 - x_3)] , \\
B_{\text{t}} &= A_{\text{t}} + z_{\text{ver}} , \\
z_{\text{box};\text{u}} &= z_{\text{box};\text{t}}|_{t \rightarrow u} .
\end{aligned} \tag{C.4}$$

The acnode integrals are easy to evaluate numerically in the physical region for the reaction $\gamma\gamma \rightarrow \pi\pi$, because branch points occur at $t = 4, u = 4$ only.

On the other hand, the vertex and box integrals contain branch points at $s = 4$. In order to evaluate these integrals at $s \geq 4$, we invoke dispersion relations in the manner described in [10].

D The polynomials P_A and P_B

Here, we display the polynomials $P_{A(B)}$ that occur in the expressions $\Delta_{A(B)}$ in Appendix C. We use the abbreviations

$$\begin{aligned}
x_+ &= x_1 + x_2 - 2 x_1 x_2, \ x_- = x_1 - x_2, \\
x_{123} &= (1 + x_3 - 2 x_2 x_3)(1 - x_3 + 2 x_1 x_2 x_3) .
\end{aligned} \tag{D.1}$$

D.1 The polynomials P_A

$$P_{A;\text{acn}}^{(0)} = -192 x_3 (1 - x_3)(s x_+ - \nu x_-),$$

$$\begin{aligned} P_{A;\text{acn}}^{(1)} = & -6 s \nu x_- (1 - x_3) \\ & \times \left[1 + 8 x_3^3 + 3 x_3^4 - 4 x_+ (x_3 + 3 x_3^3 + 2 x_3^4) + 2 x_-^2 (1 + 2 x_3^3 - 3 x_3^4) \right] \\ & - 6 s^2 (1 - x_3) \left[x_+^2 (1 + 2 x_3 + 14 x_3^3 + 7 x_3^4) + 6 x_-^2 x_3^4 \right. \\ & \left. - x_+ \left(1 + 2 x_-^2 + 4 x_3^3 (2 + x_-^2) + 3 x_3^4 (1 + 2 x_-^2) \right) \right] \\ & + 6 \nu^2 x_-^2 (1 - x_3) \left[1 - 2 x_3 + 2 x_3^3 + 5 x_3^4 - 12 x_+ x_3^4 \right] \\ & + 12 s \left[-2 x_+^2 (1 - x_3)^3 (1 + 2 x_3 + 3 x_3^2) \right. \\ & + x_3 (2 + 33 x_3 - 19 x_3^2 - 19 x_3^3 + 15 x_3^4) \\ & + x_+ (-4 + 2 x_3 - 63 x_3^2 + 25 x_3^3 + 51 x_3^4 - 35 x_3^5) \\ & \left. + 2 x_-^2 x_3 (2 + 9 x_3 - 7 x_3^2 + 5 x_3^3 - 3 x_3^4) \right] \\ & + 12 \nu x_- (1 - x_3) \left[4 - 2 x_3 - 5 x_3^2 - 4 x_3^3 + 19 x_3^4 \right. \\ & \left. + 2 x_+ (1 + 8 x_3^3 - 21 x_3^4) \right] \\ & - 48 x_3 \left[4 + 4 x_3 + 6 x_3^2 - 19 x_3^3 + 10 x_3^4 \right. \\ & \left. + x_+ (2 - 3 x_3 - 19 x_3^2 + 41 x_3^3 - 21 x_3^4) \right], \end{aligned}$$

$$\begin{aligned} P_{A;\text{acn}}^{(2)} = & 2 s \nu x_- (1 - x_3)^2 \left[-11 - 8 x_3 - 8 x_3^2 - 24 x_3^3 - 9 x_3^4 \right. \\ & + 12 x_+ (4 + x_3 + 3 x_3^3 + 2 x_3^4) - 2 x_-^2 (11 + 8 x_3 + 8 x_3^2 + 6 x_3^3 - 9 x_3^4) \left. \right] \\ & - 2 s^2 (1 - x_3)^2 \left[x_+^2 (35 - 18 x_3 + 34 x_3^3 + 21 x_3^4) + 18 x_-^2 x_3^4 \right. \\ & \left. - x_+ \left(11 + 16 x_3^3 + 9 x_3^4 + 2 x_-^2 (11 - 2 x_3^3 + 9 x_3^4) \right) \right] \\ & + 2 \nu^2 x_-^2 (1 - x_3)^2 \left[-13 + 18 x_3 - 2 x_3^3 + (15 - 36 x_+) x_3^4 \right] \\ & + 4 s (1 - x_3) \left[x_3 (22 + 11 x_3 + 83 x_3^2 - 101 x_3^3 + 45 x_3^4) \right. \\ & - 2 x_+^2 (1 - x_3)^2 \left(11(1 + x_3 + x_3^2) - 9 x_3^3 \right) \\ & + x_+ (60 - 178 x_3 + 43 x_3^2 - 173 x_3^3 + 233 x_3^4 - 105 x_3^5) \\ & \left. + 2 x_-^2 (2 - x_3) x_3 \left(11(1 + x_3 + x_3^2) + 9 x_3^3 \right) \right] \\ & + 4 \nu x_- (1 - x_3)^2 \left[-60 + 74 x_3 + 9 x_3^2 - 56 x_3^3 + 57 x_3^4 \right. \\ & \left. + x_+ (22 + 104 x_3^3 - 126 x_3^4) \right] \\ & + 16 x_3 (1 - x_3) \left[60 + 18 x_3 - 108 x_3^2 + 93 x_3^3 - 30 x_3^4 \right. \\ & \left. + x_+ (-22 - 83 x_3 + 205 x_3^2 - 187 x_3^3 + 63 x_3^4) \right], \end{aligned}$$

$$P_{A; \text{ver}} = 128 s x_2^2 (1 - 2 x_2) x_3^4 [3 - 2 x_2 (2 - 15 x_3) x_3 - 18 x_3^2 - 15 x_2^2 x_3^2] \\ - 32 s^2 x_2^2 (1 - 2 x_2) (30 - 42 x_2 + 7 x_2^2) x_3^6,$$

$$P_{A; \text{box}_+}^{(1)} = -96 s x_2 x_3^2 [-6 + 9 x_3 + 20 x_2 x_3 - 22 x_1 x_2 x_3 \\ - 2 x_3^2 - 40 x_2 x_3^2 + 6 x_1 x_2 x_3^2 - 4 x_2^2 x_3^2 + 52 x_1 x_2^2 x_3^2 - 8 x_1^2 x_2^2 x_3^2 \\ - 15 x_3^3 + 58 x_2 x_3^3 + 14 x_1 x_2 x_3^3 - 12 x_2^2 x_3^3 - 72 x_1 x_2^2 x_3^3 - 2 x_1^2 x_2^2 x_3^3 \\ + 8 x_1 x_2^3 x_3^3 + 4 x_1^2 x_2^3 x_3^3 + 20 x_3^4 - 48 x_2 x_3^4 - 36 x_1 x_2 x_3^4 + 20 x_2^2 x_3^4 \\ + 76 x_1 x_2^2 x_3^4 + 10 x_1^2 x_2^2 x_3^4 - 24 x_1 x_2^3 x_3^4 - 24 x_1^2 x_2^3 x_3^4 + 24 x_1^2 x_2^4 x_3^4] \\ - 16 s^2 x_2^2 x_3^4 [12 + 12 x_1 - 12 x_2 - 24 x_1 x_2 + 12 x_1^2 x_2 + 30 x_1 x_3 \\ - 24 x_2 x_3 - 90 x_1 x_2 x_3 + 27 x_1^2 x_2 x_3 + 30 x_2^2 x_3 + 66 x_1 x_2^2 x_3 \\ - 24 x_1^2 x_2^2 x_3 - 10 x_1^3 x_2^2 x_3 - 24 x_3^2 + 6 x_1 x_3^2 + 66 x_2 x_3^2 - 18 x_1 x_2 x_3^2 \\ + 45 x_1^2 x_2 x_3^2 - 48 x_2^2 x_3^2 + 48 x_1 x_2^2 x_3^2 - 120 x_1^2 x_2^2 x_3^2 - 28 x_1^3 x_2^2 x_3^2 \\ - 24 x_1 x_2^3 x_3^2 + 36 x_1^2 x_2^3 x_3^2 + 56 x_1^3 x_2^3 x_3^2] \\ + 48 \nu^2 x_2^3 x_3^4 [-4 + 8 x_1 - 8 x_1^2 + 2 x_1 x_3 + 7 x_1^2 x_3 + 10 x_2 x_3 \\ - 30 x_1 x_2 x_3 + 30 x_1^2 x_2 x_3 - 10 x_1^3 x_2 x_3 + 6 x_3^2 - 14 x_1 x_3^2 + 3 x_1^2 x_3^2 \\ - 12 x_2 x_3^2 + 12 x_1 x_2 x_3^2 + 12 x_1^2 x_2 x_3^2 - 12 x_1^3 x_2 x_3^2 + 24 x_1 x_2^2 x_3^2 \\ - 48 x_1^2 x_2^2 x_3^2 + 24 x_1^3 x_2^2 x_3^2] \\ + 384 x_2 x_3^2 [-6 + 9 x_3 + 19 x_2 x_3 - 19 x_1 x_2 x_3 + 7 x_3^2 - 50 x_2 x_3^2 \\ - 2 x_1 x_2 x_3^2 + 52 x_1 x_2^2 x_3^2 - 15 x_3^3 + 44 x_2 x_3^3 + 16 x_1 x_2 x_3^3 \\ - 60 x_1 x_2^2 x_3^3 + 8 x_3^4 - 16 x_2 x_3^4 - 16 x_1 x_2 x_3^4 + 32 x_1 x_2^2 x_3^4],$$

$$P_{A; \text{box}_+}^{(2)} = -24 s \nu^2 (1 - x_1)^2 x_2^3 (1 + x_2 + x_1 x_2 - 2 x_1 x_2^2) x_3^6 x_{123} \\ + 96 s x_2 x_3^4 x_{123} [-7 x_2 - 7 x_1 x_2 + 14 x_1 x_2^2 + 3 x_3 + 6 x_2 x_3 \\ + 6 x_1 x_2 x_3 - 12 x_1 x_2^2 x_3 - 3 x_3^2 - 2 x_2 x_3^2 - 2 x_1 x_2 x_3^2 + 4 x_1 x_2^2 x_3^2] \\ - 48 s^2 x_2^2 x_3^4 x_{123} [-2 - 2 x_1 - x_2 + 6 x_1 x_2 - x_1^2 x_2 + 3 x_3 + 3 x_1 x_3 \\ - 6 x_1 x_2 x_3 - 4 x_3^2 - 4 x_1 x_3^2 + 2 x_2 x_3^2 + 8 x_1 x_2 x_3^2 \\ + 2 x_1^2 x_2 x_3^2 - 4 x_1 x_2^2 x_3^2 - 4 x_1^2 x_2^2 x_3^2 + 4 x_1^2 x_2^3 x_3^2] \\ - 24 s^3 x_2^3 (1 + x_1 - 2 x_1 x_2) (1 + x_1 - x_2 - x_1^2 x_2) x_3^6 x_{123} \\ - 48 \nu^2 (1 - x_1)^2 x_2^3 (1 - x_3) x_3^4 (1 + 4 x_3) x_{123} + 2 x_2 (1 - x_3)^2 x_3^4 x_{123},$$

$$P_{A; \text{box}_-}^{(1)} = -32 s \nu x_2^2 x_3^4 [-6 + 6 x_1 + 12 x_1 x_2 - 18 x_1^2 x_2 \\ - 15 x_1 x_3 + 12 x_2 x_3 + 33 x_1^2 x_2 x_3 - 30 x_1 x_2^2 x_3 + 21 x_1^2 x_2^2 x_3 \\ - 10 x_1^3 x_2^2 x_3 + 12 x_3^2 + 3 x_1 x_3^2 - 24 x_2 x_3^2 - 30 x_1 x_2 x_3^2 \\ + 18 x_1^2 x_2 x_3^2 + 6 x_2^2 x_3^2 + 54 x_1 x_2^2 x_3^2 - 48 x_1^2 x_2^2 x_3^2 + 4 x_1^3 x_2^2 x_3^2]$$

$$\begin{aligned}
& -96 \nu x_2^2 x_3^3 [-9 + 11 x_1 + 12 x_3 - 14 x_1 x_3 + 24 x_2 x_3 \\
& -56 x_1 x_2 x_3 + 28 x_1^2 x_2 x_3 + 15 x_3^2 - 27 x_1 x_3^2 - 58 x_2 x_3^2 \\
& +84 x_1 x_2 x_3^2 + 8 x_1^2 x_2 x_3^2 + 60 x_1 x_2^2 x_3^2 - 80 x_1^2 x_2^2 x_3^2 \\
& -16 x_3^3 + 28 x_1 x_3^3 + 32 x_2 x_3^3 - 20 x_1 x_2 x_3^3 - 42 x_1^2 x_2 x_3^3 \\
& -64 x_1 x_2^2 x_3^3 + 84 x_1^2 x_2^2 x_3^3],
\end{aligned}$$

$$\begin{aligned}
P_{\text{A}; \text{box}_-}^{(2)} &= 48 s \nu (1 - x_1) x_2^2 x_3^4 x_{123} \\
&\times \left[-2 + 3 x_3 + 3 x_2 x_3 + 3 x_1 x_2 x_3 - 6 x_1 x_2^2 x_3 - 4 x_3^2 \right. \\
&\quad \left. - 2 x_2 x_3^2 - 2 x_1 x_2 x_3^2 + 4 x_1 x_2^2 x_3^2 \right] \\
&+ 24 s^2 \nu (1 - x_1^2) x_2^3 (2 - x_2 - x_1 x_2) x_3^6 x_{123} \\
&+ \nu (1 - x_1) x_2^2 (1 - x_3) x_3^4 (1 - 2 x_3) x_{123} \\
&+ 24 \nu^3 (1 - x_1)^3 x_2^4 x_3^6 x_{123}.
\end{aligned}$$

D.2 The polynomials P_B

$$\begin{aligned}
P_{\text{B}; \text{acn}}^{(0)} &= 96 x_3 (1 - x_3) \left[\frac{\nu}{s} x_- - x_+ \right], \\
P_{\text{B}; \text{acn}}^{(1)} &= \frac{6 \nu}{s} x_- \left[4 - 2 x_3 + 21 x_3^2 - 19 x_3^3 + 3 x_3^4 + 5 x_3^5 \right] \\
&\quad - \frac{3 \nu^2}{s} x_-^2 (1 - x_3) [1 + 2 x_3 + 2 x_3^3 + x_3^4] \\
&\quad - \frac{24}{s} x_3 (2 - x_3^2) [2 - 8 x_3 + 5 x_3^2] + 3 s (1 - x_3) \\
&\quad \times \left[x_+^2 (1 - x_3)^3 (1 + x_3) - x_+ (1 + 8 x_3^3 + 3 x_3^4) + 6 x_-^2 x_3^4 \right] \\
&\quad + 6 \left[x_+ (1 - x_3)^2 (-4 - 2 x_3 - 3 x_3^2 + 13 x_3^3) \right. \\
&\quad \left. + x_3 (-2 - 33 x_3 + 19 x_3^2 + 19 x_3^3 - 15 x_3^4) \right],
\end{aligned}$$

$$\begin{aligned}
P_{\text{B}; \text{acn}}^{(2)} &= -\frac{2 \nu}{s} x_- (1 - x_3) \\
&\times \left[-34 + 152 x_3 - 43 x_3^2 + 21 x_3^3 - 27 x_3^4 + 15 x_3^5 \right] \\
&\quad - \frac{\nu^2}{s} x_-^2 (1 - x_3)^2 [35 - 18 x_3 - 2 x_3^3 + 3 x_3^4] \\
&\quad + \frac{8}{s} x_3 (1 - x_3) [34 - 67 x_3 + 95 x_3^2 - 56 x_3^3 + 15 x_3^4] \\
&\quad - s (1 - x_3)^2 [x_+^2 (1 - x_3)^2 (13 + 8 x_3 + 3 x_3^2) \\
&\quad + x_+ (11 + 16 x_3^3 + 9 x_3^4) - 18 x_-^2 x_3^4]
\end{aligned}$$

$$\begin{aligned}
& +\nu x_-(1-x_3)^2 \left[11+16x_3^3+9x_3^4+12x_+(4-3x_3-x_3^4) \right] \\
& +2(1-x_3) \left[-x_3(22+11x_3+83x_3^2-101x_3^3+45x_3^4) \right. \\
& \left. +x_+(34-108x_3+65x_3^2+73x_3^3-103x_3^4+39x_3^5) \right],
\end{aligned}$$

$$\begin{aligned}
P_{\text{B}; \text{ver}} &= 16s x_2^2(1-2x_2)x_3^5 \left[33x_2^2x_3-6(4-5x_3)-2x_2(4+9x_3) \right] \\
&-1536x_2^2(1-2x_2)(1-x_3)(1-2x_3)x_3^4,
\end{aligned}$$

$$\begin{aligned}
P_{\text{B}; \text{box}_+}^{(1)} &= -\frac{24\nu^2}{s} x_2^3(1-x_3)x_3^4 \left[4+8x_1-10x_3-2x_1x_3-3x_1^2x_3 \right] \\
&- \frac{1152}{s} x_2(1-x_3)^2 x_3^2(1-2x_3+2x_3^2) \\
&-24s x_2^2 x_3^4 \left[4+12x_1-4x_2-12x_3-14x_1x_3+10x_2x_3 \right. \\
&-14x_1x_2x_3+17x_1^2x_2x_3-14x_1^2x_2^2x_3+8x_3^2-2x_1x_3^2-6x_2x_3^2 \\
&+14x_1x_2x_3^2-3x_1^2x_2x_3^2+4x_1x_2^2x_3^2-12x_1^2x_2^2x_3^2+12x_1^2x_2^3x_3^2 \left. \right] \\
&-48x_2(1-x_3)x_3^2 \left[-6+19x_3+16x_1x_2x_3-27x_3^2-2x_2x_3^2 \right. \\
&-18x_1x_2x_3^2-28x_1x_2^2x_3^2+20x_3^3-32x_1x_2x_3^3+64x_1x_2^2x_3^3 \left. \right],
\end{aligned}$$

$$\begin{aligned}
P_{\text{B}; \text{box}_+}^{(2)} &= -\frac{24\nu^2}{s} (1-x_1)^2 x_2^3(1-x_3)^3 x_3^4(1+4x_3) \\
&+ \frac{1}{s} x_2(1-x_3)^4 x_3^4 \\
&-24s x_2^2(1-x_3)^2 x_3^4 \left[-2-2x_1-x_2+6x_1x_2-x_1^2x_2 \right. \\
&+3x_3+3x_1x_3-6x_1x_2x_3-4x_3^2-4x_1x_3^2+2x_2x_3^2 \\
&+8x_1x_2x_3^2+2x_1^2x_2x_3^2-4x_1x_2^2x_3^2-4x_1^2x_2^2x_3^2+4x_1^2x_2^3x_3^2 \left. \right] \\
&-12s^2 x_2^3(1+x_1-2x_1x_2)(1+x_1-x_2-x_1^2x_2)(1-x_3)^2 x_3^6 \\
&+12\nu^2(1-x_1)^2 x_2^3(-1-x_2-x_1x_2+2x_1x_2^2)(1-x_3)^2 x_3^6 \\
&+48x_2(1-x_3)^2 x_3^4 \left[-7x_2-7x_1x_2+14x_1x_2^2+3x_3 \right. \\
&+6x_2x_3+6x_1x_2x_3-12x_1x_2^2x_3-3x_3^2-2x_2x_3^2 \\
&-2x_1x_2x_3^2+4x_1x_2^2x_3^2 \left. \right],
\end{aligned}$$

$$\begin{aligned}
P_{\text{B}; \text{box}_-}^{(1)} &= \frac{48\nu}{s} x_2^2(1-x_3)^2 x_3^3(5+11x_1-28x_3-4x_1x_3) \\
&+48\nu x_2^2 x_3^4 \left[2+2x_1+8x_1x_2-6x_3-3x_1x_3-2x_2x_3 \right. \\
&-4x_1x_2x_3+3x_1^2x_2x_3-12x_1x_2^2x_3-3x_1^2x_2^2x_3+4x_3^2 \\
&+x_1x_3^2+2x_2x_3^2-10x_1x_2x_3^2+18x_1x_2^2x_3^2 \left. \right],
\end{aligned}$$

$$P_{\text{B}; \text{box}_-}^{(2)} = \frac{144\nu}{s} (1-x_1)x_2^2(1-x_3)^3 x_3^4(1-2x_3)$$

$$\begin{aligned}
& + \frac{12 \nu^3}{s} (1 - x_1)^3 x_2^4 (1 - x_3)^2 x_3^6 \\
& - 12 s \nu (1 - x_1^2) x_2^3 (-2 + x_2 + x_1 x_2) (1 - x_3)^2 x_3^6 \\
& + 24 \nu (1 - x_1) x_2^2 (1 - x_3)^2 x_3^4 [-2 + 3 x_3 + 3 x_2 x_3 + 3 x_1 x_2 x_3 \\
& - 6 x_1 x_2^2 x_3 - 4 x_3^2 - 2 x_2 x_3^2 - 2 x_1 x_2 x_3^2 + 4 x_1 x_2^2 x_3^2] .
\end{aligned}$$

References

- [1] J. Gasser and H. Leutwyler, *Annals Phys.* **158** (1984) 142.
- [2] J. Gasser and H. Leutwyler, *Nucl. Phys. B* **250** (1985) 465.
- [3] J. Bijnens and F. Cornet, *Nucl. Phys. B* **296** (1988) 557.
- [4] J. F. Donoghue, B. R. Holstein and Y. C. Lin, *Phys. Rev. D* **37** (1988) 2423 .
- [5] S. Bellucci, J. Gasser and M. E. Sainio, *Nucl. Phys. B* **423** (1994) 80
[Erratum-ibid. B **431** (1994) 413] [arXiv:hep-ph/9401206].
- [6] U. Burgi, *Nucl. Phys. B* **479** (1996) 392 [arXiv:hep-ph/9602429];
U. Burgi, *Phys. Lett. B* **377** (1996) 147 [arXiv:hep-ph/9602421].
- [7] H. W. Fearing and S. Scherer, *Phys. Rev. D* **53** (1996) 315
[arXiv:hep-ph/9408346].
- [8] J. Bijnens, G. Colangelo and G. Ecker, *JHEP* **9902** (1999) 020
[arXiv:hep-ph/9902437].
- [9] J. Bijnens, G. Colangelo and G. Ecker, *Annals Phys.* **280** (2000) 100
[arXiv:hep-ph/9907333].
- [10] J. Gasser and M. E. Sainio, *Eur. Phys. J. C* **6** (1999) 297
[arXiv:hep-ph/9803251].
- [11] I. Guiasu and E. E. Radescu, *Annals Phys.* **120** (1979) 145; *ibid.* **122** (1979) 436.
- [12] L. V. Fil'kov and V. L. Kashevarov, arXiv:nucl-th/0505058.
- [13] J. Ahrens *et al.*, *Eur. Phys. J. A* **23** (2005) 113 [arXiv:nucl-ex/0407011].
- [14] The COMPASS Collaboration, CERN Proposal CERN/SPSLC 96-14, SPSC/P 297, March 1, 1996, and Addendum 1, CERN/SPSLC 96-30, SPSC/P 297, March 20, 1996
[http://wwwcompass.cern.ch/compass/proposal/welcome.html].
- [15] M. Moinester [for the COMPASS Collaboration], Workshop *Symmetries and Spin*-Prague-SPIN-2002, Advanced Study Institute, INTAS monitoring Conference, Prague, 14-24 July, 2002, *Czech. J. Phys.* **53** (2003) B169 [arXiv:hep-ex/0301024].

- [16] J. Gasser, M.A. Ivanov, M.E. Sainio, work in progress.
- [17] G. Colangelo, J. Gasser and H. Leutwyler, Nucl. Phys. B **603** (2001) 125 [arXiv:hep-ph/0103088].
- [18] J. Bijnens and P. Talavera, Nucl. Phys. B **489** (1997) 387 [arXiv:hep-ph/9610269].
- [19] M. Knecht, B. Moussallam and J. Stern, Nucl. Phys. B **429** (1994) 125 [arXiv:hep-ph/9402318].
- [20] B. R. Holstein, Phys. Lett. B **244** (1990) 83.
- [21] S. Descotes-Genon and B. Moussallam, arXiv:hep-ph/0505077.
- [22] J. A. M. Vermaseren, arXiv:math-ph/0010025.
- [23] U. Burgi, Ph. D. thesis, University of Bern, 1996.
- [24] L. V. Fil'kov and V. L. Kashevarov, Eur. Phys. J. A **5** (1999) 285 [arXiv:nucl-th/9810074].
- [25] A. E. Kaloshin, V. M. Persikov and V. V. Serebryakov, Phys. Atom. Nucl. **57** (1994) 2207 [Yad. Fiz. **57N12** (1994) 2298] [arXiv:hep-ph/9402220].
- [26] R. Baldini, S. Bellucci, Proc. Workshop on Chiral Dynamics: Theory and Experiments, Cambridge, MA, USA, 25-29 July, 1994, Lecture Notes in Physics 452 (Springer Berlin, A.M. Bernstein, B.R. Holstein (eds.)), p.177; S. Bellucci, arXiv:hep-ph/9508282; D. Babusci, S. Bellucci, G. Giordano and G. Matone, Phys. Lett. B **314** (1993) 112; D. Babusci, S. Bellucci, G. Giordano, G. Matone, A. M. Sandorfi and M. A. Moinester, Phys. Lett. B **277** (1992) 158.
- [27] G. Ecker, J. Gasser, H. Leutwyler, A. Pich and E. de Rafael, Phys. Lett. B **223** (1989) 425; G. Ecker, J. Gasser, A. Pich and E. de Rafael, Nucl. Phys. B **321** (1989) 311; M. Knecht and A. Nyffeler, Eur. Phys. J. C **21** (2001) 659 [arXiv:hep-ph/0106034]; V. Cirigliano, G. Ecker, M. Eidemuller, R. Kaiser, A. Pich and J. Portoles, JHEP **0504** (2005) 006 [arXiv:hep-ph/0503108].